Advances in Materials Research, *Vol. 8, No. 3 (2019) 179-196*
DOI: https://doi.org/10.12989/amr.2019.8.3.179

Analysis of static and dynamic characteristics of strain gradient shell structures made of porous nano-crystalline materials

Luay Badr Hamad, Basima Salman Khalaf and Nadhim M. Faleh*

Al-Mustansiriah University, Engineering Collage P.O. Box 46049, Bab-Muadum, Baghdad 10001, Iraq

(*Received July 28, 2019, Revised September 28, 2019, Accepted October 20, 2019*)

Abstract. This paper researches static and dynamic bending behaviors of a crystalline nano-size shell having pores and grains in the framework of strain gradient elasticity. Thus, the nanoshell is made of a multi-phase porous material for which all material properties on dependent on the size of grains. Also, in order to take into account small size effects much accurately, the surface energies related to grains and pores have been considered. In order to take into account all aforementioned factors, a micro-mechanical procedure has been applied for describing material properties of the nanoshell. A numerical trend is implemented to solve the governing equations and derive static and dynamic deflections. It will be proved that the static and dynamic deflections of the crystalline nanoshell rely on pore size, grain size, pore percentage, load location and strain gradient coefficient.

Keywords: crystalline material; static bending; porous nanoshell; strain gradient; Mori-Tanaka scheme

1. Introduction

Silicon is a basic material used in sensing systems and structures which may have macro, micron or nano dimensions. This material has not a perfect and ideal structure and it may possess small size pores. Pores or voids in material texture of silicon leads to the variation in material attributes. Also, grains are possible to be created within silicon and hence this type of material would be a crystalline material. Actually, the crystalline materials have grains or crystals of silicone together with voids and an interface zone between the grains and voids (Wang *et al*. 2003). The distribution of grains and voids within material structure would be random and it is not possible to place them in prescribed locations. In fact, the grains growth in possible positions during the fabrication of crystalline materials. Moreover, if the dimensions of grains are reduced to nano scales, the material would be a nanocrystalline material (Meyers *et al*. 2006). There are diverse approaches for describing material properties of nanocrystalline materials (Zhou *et al*. 2013) having grains and voids.

Shell structures have great application in mechanical devices and system form macro to micro/nano dimensions. Macro size shells are extensively researched via classic elasticity theory in the view of structural dynamic analysis. However, classic elasticity theory is not appropriate for nano dimension shells for which small scale impacts exist. Thus, another theories to carry out size-

*Corresponding author, Professor, E-mail: dr.nadhim@uomustansiriyah.edu.iq

http://www.techno-press.org/?journal=amr&subpage=5 ISSN: 2234-0912 (Print), 2234-179X (Online)

dependent dynamical analysis of nano dimension structural components are strain gradient and nonlocal elasticity theories (Aydogdu 2009, Thai 2012, Ke *et al*. 2012, Eltaher *et al*. 2013, Barati 2017, Al-Maliki *et al*. 2019, Ahmed *et al*. 2019). Nonlocal elastic theory were used by various authors in order to incorporate small scale impacts in analysis of nanostructures based on a single scale factor (Lim 2010, Li 2014a, b, Li *et al*. 2013, Zenkour and Abouelregal 2014, Ebrahimi and Barati 2016, 2017a, Barati and Shahverdi 2016, 2017a, Bounouara *et al*. 2016, Besseghier *et al*. 2017, Mokhtar *et al*. 2018). The scale factor defined by nonlocal elastic theory leads to structural rigidity reduction which highlights that nano size structures have different mechanical performance from macro scale counterparts. One another scale factor is defined by strain gradient theory leading to structural rigidity increment. The strain gradient theory express that the strains are not uniform within the material structures. Therefore, this theory would be useful for modeling of nanocrystalline materials and structures. For various types of materials and structures, the strain gradient theory has shown its efficacy (Lim *et al*. 2015, Li *et al*. 2016, Mehralian *et al*. 2017, Barati and Shahverdi 2017b).

Mechanical analysis of nanocrystalline structures has been carried out by few researches. Especially nanocrysalline nanoshells having nano-size grains and pores are not studied before. However, some papers are published on nanocrystalline nanoplates and nanobeams based on strain gradient theory taking into account the size of pores and grains (Ebrahimi and Barati 2017b, 2018, Barati and Shahverdi 2017c, d). For other types of materials rather than nanocrystalline materials, some researchers studied the mechanical properties of elastic nanoshells based on nonlocal and strain gradient theories and proved the efficacy of the theories (Zaera *et al*. 2013, Ke *et al*. 2014, Mehralian *et al*. 2016, Farajpour *et al*. 2017, Sun *et al*. 2016).

The present article studies static and dynamic bending behaviors of a crystalline nano-size shell having pores and grains in the framework of strain gradient elasticity. Thus, the nanoshell is made of a multi-phase porous material for which all material properties on dependent on the size of grains. Also, in order to take into account small size effects much accurately, the surface energies related to grains and pores have been considered. In order to take into account all aforementioned factors, a micro-mechanical procedure has been applied for describing material properties of the nanoshell. A numerical trend is implemented to solve the governing equations and derive static and dynamic deflections. It will be proved that the static and dynamic deflections of the crystalline nanoshell rely on pore size, grain size, pore percentage, load location and strain gradient coefficient.

2. Model of nanocrystalline nanoshells

Figs. 1 and 2 illustrate a nanocrystalline nanoshell made of silicone under radial dynamic load with specific frequency. The figures clearly show that pores are available in the material structure and are able to change material properties. Elastic properties (Young's moduli and Poisson's ratio) for a nanocrystalline nanoshell can be described as functions of bulk and shear moduli (K_{NcM}, μ_{NcM}) as

$$E_{NcM} = \frac{9K_{NcM}\mu_{NcM}}{3K_{NcM} + \mu_{NcM}} \tag{1}$$

$$v_{NcM} = \frac{3K_{NcM} - 2\mu_{NcM}}{2(3K_{NcM} + \mu_{NcM})} \tag{2}$$

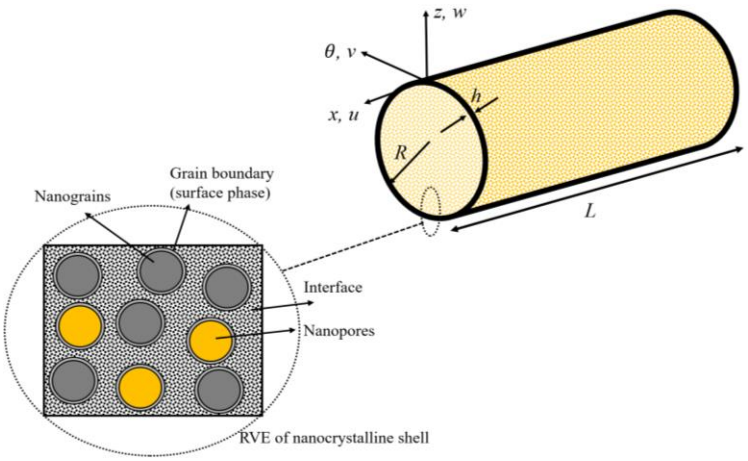

Fig. 1 A crystalline nanoshell with pores and grains

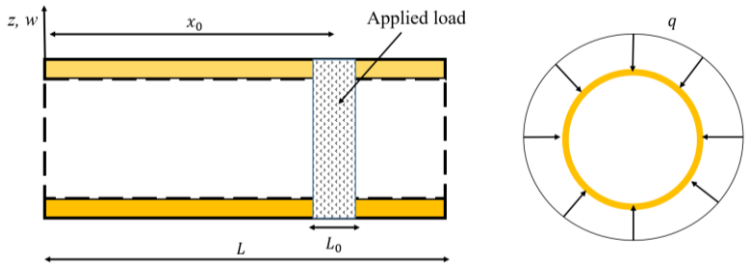

Fig. 2 The cylindrical nanoshell under radial loading

So that

$$K_{NcM} \cong k_{H_1} \times k_{H_2} \times \frac{1}{\eta k_g} \tag{3}$$

$$\mu_{NcM} \cong \mu_{H_1} \times \mu_{H_2} \times \frac{1}{\eta \mu_g} \tag{4}$$

So that $\eta = E_{in}/E_g$ and also

$$k_{H_1} = k_{eff}(k_{in} = \eta k_g, \mu_{in} = \eta \mu_g, k_g, \mu_g, f_g, k_g^s, \mu_g^s, v_{in} = v_g, R_g) \tag{5a}$$

$$\mu_{H_1} = \mu_{eff}(k_{in} = \eta k_g, \mu_{in} = \eta \mu_g, k_g, \mu_g, f_g, k_g^s, \mu_g^s, v_{in} = v_g, R_g) \tag{5b}$$

$$k_{H_2} = k_{eff}(k_{in} = \eta k_g, \mu_{in} = \eta \mu_g, k_g = 0, \mu_g = 0, f_v, k_v^s, \mu_v^s, v_v, R_v) \tag{5c}$$

$$\mu_{H_2} = \mu_{eff}(k_{in} = \eta k_g, \mu_{in} = \eta \mu_g, k_g = 0, \mu_g = 0, f_v, k_v^s, \mu_v^s, v_v, R_v) \tag{5d}$$

In above relations g denotes the nano-grains material properties. Also, v denote the porosities

material properties. So, f_g and f_v are grain and pores volume fractions defined as

$$f_g = r(1-f_v), r = \frac{R_g^3}{(R_g+T_{in})^3} \tag{6}$$

Here, $R_g, R_v$and T_{in} respectively denote the main radiuses of nano-grain, nano-porosity and interface thickness. Above equations are employed in order to characterize all material properties including nano-porosity effect. Without including nano-porosity effect, the material properties (Bulk and shear moduli) become (Ebrahimi and Barati 2017b)

$$k_{eff} = \frac{3k_g\left(4f_g\mu_{in}+3k_{in}\right)+2\mu_{in}\left(4f_g\mu_{in}k_s^*+3k_{in}\left(2-2f_g+k_s^*\right)\right)}{3\left(3\left(1-f_g\right)k_g+3f_gk_{in}+2\mu_{in}\left(2+k_s^*-f_gk_s^*\right)\right)} \tag{7}$$

$$\mu_{eff} = \frac{\mu_{in}\left(5-8f_g\xi_3(7-5v_{in})\right)}{5-f_g(5-84\xi_1-20\xi_2)} \tag{8}$$

So that

$$\xi_1 = \frac{15(1-v_{in})(k_s^*+2\mu_s^*)}{4H} \tag{9a}$$

$$\xi_2 = \frac{-15(1-v_{in})(\left(\frac{\mu_g}{\mu_{in}}\right)(7+5v_g)-8v_g(5+3k_s^*+\mu_s^*)+7(4+3k_s^*+2\mu_s^*))}{4H} \tag{9b}$$

$$\begin{aligned}\xi_3 = \frac{5}{16H}\Bigg[&2\left(\frac{\mu_g}{\mu_{in}}\right)^2(7+5v_g)-4(7-10v_g)(2+k_s^*)(1-\mu_s^*)\\&+\left(\frac{\mu_g}{\mu_{in}}\right)(7(6+5k_s^*+4\mu_s^*)-v_g(90+47k_s^*+4\mu_s^*))\Bigg]\end{aligned} \tag{9c}$$

and

$$\begin{aligned}H = &-2\left(\frac{\mu_g}{\mu_{in}}\right)^2(7+5v_g)(4-5v_{in})+7\left(\frac{\mu_g}{\mu_{in}}\right)\begin{pmatrix}-39-20k_s^*-16\mu_s^*\\+5v_g(9+5k_s^*+4\mu_s^*)\end{pmatrix}\\&+\left(\frac{\mu_g}{\mu_{in}}\right)v_g\left(285+188k_s^*+16\mu_s^*-5v_{in}(75+47k_s^*+4\mu_s^*)\right)\\&+4(7-10v_g)(-7-11\mu_s^*-k_s^*(5+4\mu_s^*)+v_{in}(5+13\mu_s^*+k_s^*(4+5\mu_s^*)))\end{aligned} \tag{9d}$$

so that $k_s^* = k_g^s/R_g\mu_{in}$ and $\mu_s^* = \mu_g^s/R_g\mu_{in}$ are surfaces bulks and shear moduli, respectively for which $k_g^s = 2(\mu_g^s+\lambda_g^s)$.

For the atoms within the material, the elastic modulus of $E(r_0)$ has been defined. This modulus is identical to that of nano-grains (E_g). r_0 is the reference position of the atoms in which they are vibrating. Then, it is possible to define elastic modulus of interface atoms as $E_{in} = E(r)$ at a new position r. Next, for the afore-mentioned elastic moduli there a relationship as follows

$$\frac{E_{in}}{E_g} = \frac{E(r)}{E(r_0)} = \frac{1}{n-m}\left((n+1)\left(\frac{r_0}{r}\right)^{n+3}-(m+1)\left(\frac{r_0}{r}\right)^{m+3}\right) \tag{10}$$

so that

$$\frac{r_0}{r} = \left(\frac{\rho(r)}{\rho(r_0)}\right)^{1/3} \tag{11}$$

Above relations are applicable to silicone when m = 8 and n = 12. Then, nanoshell mass density may be defined as follows taking into account the portions of nano-grains and nano-porosity

$$\rho_{NcM} = (1 - f_g - f_v)\rho_{in} + f_g\rho_g \tag{12}$$

Selecting first order shear deformable shell theory, the displacement field for crystalline nanoshells may be expressed by

$$u_1(x,\theta,z,t) = u(x,\theta,t) + z\varphi_x(x,\theta,t) \tag{13a}$$

$$u_2(x,\theta,z,t) = v(x,\theta,t) + z\varphi_\theta(x,\theta,t) \tag{13b}$$

$$u_3(x,\theta,z,t) = w(x,\theta,t) \tag{13c}$$

so that u,v and w define axial, circumferential and lateral components, respectively; $\varphi_x$and $\varphi_\theta$define the rotation about axial and circumferential axes.

In the framework of above shell displacements, the strain component would be

$$\begin{aligned}
\varepsilon_{xx} &= \frac{\partial u}{\partial x} + z\frac{\partial \varphi_x}{\partial x} \\
\varepsilon_\theta &= \frac{1}{R}\left(\frac{\partial v}{\partial \theta} + w + z\frac{\partial \varphi_\theta}{\partial \theta}\right) \\
\gamma_{x\theta} &= \frac{1}{R}\frac{\partial u}{\partial \theta} + \frac{\partial v}{\partial x} + \frac{z}{R}\frac{\partial \varphi_x}{\partial \theta} + z\frac{\partial \varphi_\theta}{\partial x} \\
\gamma_{zx} &= \varphi_x + \frac{\partial w}{\partial x}, \qquad \gamma_{z\theta} = \varphi_\theta + \frac{1}{R}\frac{\partial w}{\partial \theta} - \frac{v}{R}
\end{aligned} \tag{14}$$

Now, Hamilton's principle can be written as

$$\int_0^t \delta(U - T - V)dt = 0 \tag{15}$$

here, $U$is strain energy, $T$is kinetic energy and $V$is work done by external forces and

$$\delta U = \int_V (\sigma_{ij}\delta\varepsilon_{ij})Rdxd\theta dz \tag{16}$$

$$\delta V = \int_V (q_{load}))\delta wRdxd\theta dz \tag{17}$$

$$\delta K = \int_V \left(\left(\frac{\partial \delta u_1}{\partial t}\right)^2 + \left(\frac{\partial \delta u_2}{\partial t}\right)^2 + \left(\frac{\partial \delta u_3}{\partial t}\right)^2\right)Rdxd\theta dz \tag{18}$$

Also,q_{load} is radial mechanical load.

Using Hamilton's principle in Eq. (15) and Eqs. (16)-(18), the governing equations can be obtained as (Mehralian *et al*. 2017)

$$\frac{\partial N_{xx}}{\partial x}+\frac{1}{R}\frac{\partial N_{x\theta}}{\partial \theta}=I_0\frac{\partial^2 u}{\partial t^2}+I_1\frac{\partial^2 \varphi_x}{\partial t^2} \tag{19a}$$

$$\frac{\partial N_{x\theta}}{\partial x}+\frac{1}{R}\frac{\partial N_{\theta\theta}}{\partial \theta}+\frac{Q_{z\theta}}{R}=I_0\frac{\partial^2 v}{\partial t^2}+I_1\frac{\partial^2 \varphi_\theta}{\partial t^2} \tag{19b}$$

$$\frac{\partial Q_{xz}}{\partial x}+\frac{1}{R}\frac{\partial Q_{z\theta}}{\partial \theta}-\frac{N_{\theta\theta}}{R}=+I_0\frac{\partial^2 w}{\partial t^2}+q_{load} \tag{19c}$$

$$\frac{\partial M_{xx}}{\partial x}+\frac{1}{R}\frac{\partial M_{x\theta}}{\partial \theta}-Q_{xz}=I_1\frac{\partial^2 u}{\partial t^2}+I_2\frac{\partial^2 \varphi_x}{\partial t^2} \tag{19d}$$

in which

$$(I_0,I_1,I_2)=\int_{-h/2}^{h/2}(1,z,z^2)\rho_{NcM}\,dz \tag{20}$$

and

$$\{N_{xx},N_{\theta\theta},N_{x\theta}\}=\int_{-h/2}^{h/2}\{\sigma_{xx},\sigma_{\theta\theta},\sigma_{x\theta}\}\,dz \tag{21a}$$

$$\{M_{xx},M_{\theta\theta},M_{x\theta}\}=\int_{-h/2}^{h/2}\{\sigma_{xx},\sigma_{\theta\theta},\sigma_{x\theta}\}\,zdz \tag{21b}$$

$$\{Q_{xz},Q_{z\theta}\}=\kappa_s\int_{-h/2}^{h/2}\{\sigma_{xz},\sigma_{z\theta}\}\,dz \tag{21c}$$

in which $\kappa_s$is shear correction factor.

In the framework of strain gradient theory, the stress-strain relations would be

$$\begin{Bmatrix}\sigma_{xx}\\ \sigma_{\theta\theta}\\ \sigma_{x\theta}\\ \sigma_{xz}\\ \sigma_{z\theta}\end{Bmatrix}=\frac{E(z)}{1-v^2}(1-l^2\nabla^2)\begin{pmatrix}1 & v & 0 & 0 & 0\\ v & 1 & 0 & 0 & 0\\ 0 & 0 & (1-v)/2 & 0 & 0\\ 0 & 0 & 0 & (1-v)/2 & 0\\ 0 & 0 & 0 & 0 & (1-v)/2\end{pmatrix}\begin{Bmatrix}\varepsilon_{xx}\\ \varepsilon_{\theta\theta}\\ \gamma_{xy}\\ \gamma_{xz}\\ \gamma_{z\theta}\end{Bmatrix} \tag{22}$$

so that *l* is strain gradient or length scale parameter. Integrating Eq. (22) over the nanoshell thickness, the resultants presented in Eq. (21) can be obtained as

$$N_{xx}=(1-\lambda\nabla^2)\left[A_{11}\frac{\partial u}{\partial x}+B_{11}\frac{\partial \varphi_x}{\partial x}+\frac{A_{12}}{R}\left(\frac{\partial v}{\partial \theta}+w\right)+\frac{B_{12}}{R}\frac{\partial \varphi_\theta}{\partial \theta}\right] \tag{23}$$

$$M_{xx} = (1-\lambda\nabla^2)\left[B_{11}\frac{\partial u}{\partial x} + D_{11}\frac{\partial \varphi_x}{\partial x} + \frac{B_{12}}{R}\left(\frac{\partial v}{\partial \theta} + w\right) + \frac{D_{12}}{R}\frac{\partial \varphi_\theta}{\partial \theta}\right] \tag{24}$$

$$N_{\theta\theta} = (1-\lambda\nabla^2)\left[A_{12}\frac{\partial u}{\partial x} + B_{12}\frac{\partial \varphi_x}{\partial x} + \frac{A_{11}}{R}\left(\frac{\partial v}{\partial \theta} + w\right) + \frac{B_{11}}{R}\frac{\partial \varphi_\theta}{\partial \theta}\right] \tag{25}$$

$$M_{\theta\theta} = (1-\lambda\nabla^2)\left[B_{12}\frac{\partial u}{\partial x} + D_{12}\frac{\partial \varphi_x}{\partial x} + \frac{B_{11}}{R}\left(\frac{\partial v}{\partial \theta} + w\right) + \frac{D_{11}}{R}\frac{\partial \varphi_\theta}{\partial \theta}\right] \tag{26}$$

$$N_{x\theta} = (1-\lambda\nabla^2)\left[A_{66}\left(\frac{1}{R}\frac{\partial u}{\partial \theta} + \frac{\partial v}{\partial x}\right) + B_{66}\left(\frac{1}{R}\frac{\partial \varphi_x}{\partial \theta} + \frac{\partial \varphi_\theta}{\partial x}\right)\right] \tag{27}$$

$$M_{x\theta} = (1-\lambda\nabla^2)\left[B_{66}\left(\frac{1}{R}\frac{\partial u}{\partial \theta} + \frac{\partial v}{\partial x}\right) + D_{66}\left(\frac{1}{R}\frac{\partial \varphi_x}{\partial \theta} + \frac{\partial \varphi_\theta}{\partial x}\right)\right] \tag{28}$$

$$Q_{xz} = (1-\lambda\nabla^2)\tilde{A}_{66}\left(\varphi_x + \frac{\partial w}{\partial x}\right) \tag{29}$$

$$Q_{\theta z} = (1-\lambda\nabla^2)\tilde{A}_{66}\left(\varphi_\theta + \frac{1}{R}\frac{\partial w}{\partial \theta} - \frac{v}{R}\right) \tag{30}$$

in which

$$\begin{aligned}
&A_{11} = \int_{-h/2}^{h/2}\frac{E_{NcM}}{1-v^2}dz, \quad B_{11} = \int_{-h/2}^{h/2}\frac{E_{NcM}}{1-v^2}z\,dz, \quad D_{11} = \int_{-h/2}^{h/2}\frac{E_{NcM}z^2}{1-v^2}dz,\\
&A_{12} = \int_{-h/2}^{h/2}\frac{vE_{NcM}}{1-v^2}dz, \quad B_{12} = \int_{-h/2}^{h/2}\frac{vE_{NcM}}{1-v^2}z\,dz, \quad D_{12} = \int_{-h/2}^{h/2}\frac{vE_{NcM}z^2}{1-v^2}dz,\\
&A_{66} = \int_{-h/2}^{h/2}\frac{E_{NcM}}{2(1+v)}dz, \quad B_{66} = \int_{-h/2}^{h/2}\frac{E_{NcM}}{2(1+v)}zdz, \quad D_{66} = \int_{-h/2}^{h/2}\frac{E_{NcM}}{2(1+v)}z^2\,dz\\
&\tilde{A}_{66} = k_s\int_{-h/2}^{h/2}\frac{E_{NcM}}{2(1+v)}dz,
\end{aligned} \tag{31}$$

The governing equations in terms of the displacements for a crystalline nanoshell can be derived by substituting Eqs. (23)-(30), into Eq. (19) as follows

$$\begin{aligned}
&(1-\lambda\nabla^2)\left[A_{11}\frac{\partial^2 u}{\partial x^2} + B_{11}\frac{\partial^2 \varphi_x}{\partial x^2} + \frac{A_{12}}{R}\left(\frac{\partial^2 v}{\partial x\partial\theta} + \frac{\partial w}{\partial x}\right) + \frac{B_{12}}{R}\frac{\partial^2 \varphi_\theta}{\partial x\partial\theta}\right.\\
&\left.+\frac{A_{66}}{R}\left(\frac{1}{R}\frac{\partial^2 u}{\partial\theta^2} + \frac{\partial^2 v}{\partial x\partial\theta}\right) + \frac{B_{66}}{R}\left(\frac{1}{R}\frac{\partial^2 \varphi_x}{\partial\theta^2} + \frac{\partial^2 \varphi_\theta}{\partial x\partial\theta}\right)\right] - I_0\frac{\partial^2 u}{\partial t^2} - I_1\frac{\partial^2 \varphi_x}{\partial t^2} = 0
\end{aligned} \tag{32a}$$

$$\begin{aligned}
&(1-\lambda\nabla^2)\left[A_{66}\left(\frac{1}{R}\frac{\partial^2 u}{\partial x\partial\theta} + \frac{\partial^2 v}{\partial x^2}\right) + B_{66}\left(\frac{1}{R}\frac{\partial^2 \varphi_x}{\partial x\partial\theta} + \frac{\partial^2 \varphi_\theta}{\partial x^2}\right)\frac{A_{12}}{R}\frac{\partial^2 u}{\partial x\partial\theta}\right.\\
&\left.+\frac{B_{12}}{R}\frac{\partial^2 \varphi_x}{\partial x\partial\theta} + \frac{A_{11}}{R^2}\left(\frac{\partial^2 v}{\partial\theta^2} + \frac{\partial w}{\partial\theta}\right) + \frac{B_{11}}{R^2}\frac{\partial^2 \varphi_\theta}{\partial\theta^2} + \frac{\tilde{A}_{66}}{R}\left(\varphi_\theta + \frac{1}{R}\frac{\partial w}{\partial\theta} - \frac{v}{R}\right)\right]
\end{aligned} \tag{32b}$$

$$-I_0\frac{\partial^2 v}{\partial t^2}-I_1\frac{\partial^2 \varphi_\theta}{\partial t^2}=0 \tag{32b}$$

$$\begin{aligned}&(1-\lambda\nabla^2)\left[\tilde{A}_{66}\left(\frac{\partial\varphi_x}{\partial x}+\frac{\partial^2 w}{\partial x^2}\right)+\frac{\tilde{A}_{66}}{R}\left(\frac{\partial\varphi_\theta}{\partial\theta}+\frac{1}{R}\frac{\partial^2 w}{\partial\theta^2}-\frac{1}{R}\frac{\partial v}{\partial\theta}\right)\right.\\&\left.-\frac{A_{12}}{R}\frac{\partial u}{\partial x}-\frac{B_{12}}{R}\frac{\partial\varphi_x}{\partial x}-\frac{A_{11}}{R^2}\left(\frac{\partial v}{\partial\theta}+w\right)-\frac{B_{11}}{R^2}\frac{\partial\varphi_\theta}{\partial\theta}\right]-I_0\frac{\partial^2 w}{\partial t^2}=q_{load}\end{aligned} \tag{32c}$$

$$\begin{aligned}&(1-\lambda\nabla^2)\left[B_{11}\frac{\partial^2 u}{\partial x^2}+D_{11}\frac{\partial^2\varphi_x}{\partial x^2}+\frac{B_{12}}{R}\left(\frac{\partial^2 v}{\partial x\partial\theta}+\frac{\partial w}{\partial x}\right)+\frac{D_{12}}{R}\frac{\partial^2\varphi_\theta}{\partial x\partial\theta}\right.\\&\left.+\frac{B_{66}}{R}\left(\frac{1}{R}\frac{\partial^2 u}{\partial\theta^2}+\frac{\partial^2 v}{\partial x\partial\theta}\right)+\frac{D_{66}}{R}\left(\frac{1}{R}\frac{\partial^2\varphi_x}{\partial\theta^2}+\frac{\partial^2\varphi_\theta}{\partial x\partial\theta}\right)-\tilde{A}_{66}\left(\varphi_x+\frac{\partial w}{\partial x}\right)\right]\\&-I_1\frac{\partial^2 u}{\partial t^2}-I_2\frac{\partial^2\varphi_x}{\partial t^2}=0\end{aligned} \tag{32d}$$

$$\begin{aligned}&(1-\lambda\nabla^2)\left[B_{66}\left(\frac{1}{R}\frac{\partial^2 u}{\partial x\partial\theta}+\frac{\partial^2 v}{\partial x^2}\right)+D_{66}\left(\frac{1}{R}\frac{\partial^2\varphi_x}{\partial x\partial\theta}+\frac{\partial^2\varphi_\theta}{\partial x^2}\right)\right.\\&\frac{B_{12}}{R}\frac{\partial^2 u}{\partial x\partial\theta}+\frac{D_{12}}{R}\frac{\partial^2\varphi_x}{\partial x\partial\theta}+\frac{B_{11}}{R^2}\left(\frac{\partial^2 v}{\partial\theta^2}+\frac{\partial w}{\partial\theta}\right)+\frac{D_{11}}{R^2}\frac{\partial^2\varphi_\theta}{\partial\theta^2}\\&\left.-\tilde{A}_{66}\left(\varphi_\theta+\frac{1}{R}\frac{\partial w}{\partial\theta}-\frac{v}{R}\right)\right]-I_1\frac{\partial^2 v}{\partial t^2}-I_2\frac{\partial^2\varphi_\theta}{\partial t^2}=0\end{aligned} \tag{32e}$$

3. Method of solution

A numerical trend has been employed in the present research based on Galerkin's approach and also the below assumptions for displacement components (Saidi *et al*. 2016, Merazi *et al*. 2015)

$$u=\sum_{m=1}^{\infty}\sum_{n=1}^{\infty}U_{mn}\frac{\partial X_m(x)}{\partial x}cos(n\theta)\,sin(\,\omega_{ex}t) \tag{33}$$

$$v=\sum_{m=1}^{\infty}\sum_{n=1}^{\infty}V_{mn}X_m(x)\,sin(n\theta)\,sin(\,\omega_{ex}t) \tag{34}$$

$$w=\sum_{m=1}^{\infty}\sum_{n=1}^{\infty}W_{mn}X_m(x)\,cos(n\theta)\,sin(\,\omega_{ex}t) \tag{35}$$

$$\varphi_x=\sum_{m=1}^{\infty}\sum_{n=1}^{\infty}\Phi_{mn}\frac{\partial X_m(x)}{\partial x}cos(n\theta)\,sin(\,\omega_{ex}t) \tag{36}$$

$$\varphi_\theta=\sum_{m=1}^{\infty}\sum_{n=1}^{\infty}\Theta_{mn}X_m(x)\,sin(n\theta)\,sin(\,\omega_{ex}t) \tag{37}$$

The maximum values of displacements are denoted by U_{mn},V_{mn},W_{mn},Φ_{mn},Θ_{mn} and X_m is a function based on simply-supported the boundary condition. Here are the boundary conditions at $x = 0, L$ of nanoshell (Li 2014a, b, Shen *et al*. 2019)

$$w = \frac{\partial^2 w}{\partial x^2} = \frac{\partial^4 w}{\partial x^4} = 0 \tag{38}$$

By putting Eqs. (33)-(37) in Eqs. (32) and taking into account the Galerkin's concept, we obtain

$$\{[K] + \omega_{ex}^2[M]\}\begin{Bmatrix} U_{mn} \\ V_{mn} \\ W_{mn} \\ \Phi_{mn} \\ \Theta_{mn} \end{Bmatrix} = \begin{Bmatrix} 0 \\ 0 \\ Q_{load} \\ 0 \\ 0 \end{Bmatrix} \tag{39}$$

in which ω_{ex} is the excitation frequency and

$$k_{1,1} = A_{11}(\Upsilon_{31} - \lambda(\Upsilon_{51} - \frac{n^2}{R}\Upsilon_{31})) - n^2\frac{A_{66}}{R^2}\left(\Upsilon_{11} - \lambda\left(\Upsilon_{31} - \frac{n^2}{R}\Upsilon_{11}\right)\right) \tag{40}$$

$$\begin{aligned} k_{2,1} &= n\left(\frac{A_{12}}{R} + \frac{A_{66}}{R}\right)\left(\Upsilon_{11} - \lambda\left(\Upsilon_{31} - \frac{n^2}{R}\Upsilon_{11}\right)\right), \\ k_{1,2} &= -n\left(\frac{A_{12}}{R} + \frac{A_{66}}{R}\right)\left(\Upsilon_{20} - \lambda\left(\Upsilon_{40} - \frac{n^2}{R}\Upsilon_{20}\right)\right) \end{aligned} \tag{41}$$

$$\begin{aligned} k_{3,1} &= +\frac{A_{12}}{R}\left(\Upsilon_{11} - \lambda\left(\Upsilon_{31} - \frac{n^2}{R}\Upsilon_{11}\right)\right), \\ k_{1,3} &= -\frac{A_{12}}{R}\left(\Upsilon_{20} - \lambda\left(\Upsilon_{40} - \frac{n^2}{R}\Upsilon_{20}\right)\right) \end{aligned} \tag{42}$$

$$\begin{aligned} k_{4,1} &= +B_{11}\left(\Upsilon_{31} - \lambda\left(\Upsilon_{51} - \frac{n^2}{R}\Upsilon_{31}\right)\right) - n^2\frac{B_{66}}{R^2}\left(\Upsilon_{11} - \lambda\left(\Upsilon_{31} - \frac{n^2}{R}\Upsilon_{11}\right)\right), \\ k_{1,4} &= B_{11}(\Upsilon_{31} - \lambda(\Upsilon_{51} - \frac{n^2}{R}\Upsilon_{31})) - n^2\frac{B_{66}}{R^2}\left(\Upsilon_{11} - \lambda\left(\Upsilon_{31} - \frac{n^2}{R}\Upsilon_{11}\right)\right) \end{aligned} \tag{43}$$

$$k_{5,1} = n\left(\frac{B_{12}}{R} + \frac{B_{66}}{R}\right)\left(\Upsilon_{11} - \lambda\left(\Upsilon_{31} - \frac{n^2}{R}\Upsilon_{11}\right)\right), \tag{44}$$

$$k_{1,5} = -n\left(\frac{B_{66}}{R} + \frac{B_{12}}{R}\right)\left(\Upsilon_{20} - \lambda\left(\Upsilon_{40} - \frac{n^2}{R}\Upsilon_{20}\right)\right) \tag{45}$$

$$k_{2,2} = A_{66}\left(\Upsilon_{20} - \lambda\left(\Upsilon_{40} - \frac{n^2}{R}\Upsilon_{20}\right)\right) - n^2\frac{A_{11}}{R^2}\left(\Upsilon_{00} - \lambda\left(\Upsilon_{20} - \frac{n^2}{R}\Upsilon_{00}\right)\right) - \frac{\tilde{A}_{66}}{R^2}\left(\Upsilon_{00} - \lambda\left(\Upsilon_{20} - \frac{n^2}{R}\Upsilon_{00}\right)\right) \quad (46)$$

$$k_{3,2} = -n\left(\frac{A_{11}}{R^2} + \frac{\tilde{A}_{66}}{R^2}\right)\left(\Upsilon_{00} - \lambda\left(\Upsilon_{20} - \frac{n^2}{R}\Upsilon_{00}\right)\right),$$
$$k_{2,3} = -n\left(\frac{\tilde{A}_{66}}{R^2} + \frac{A_{11}}{R^2}\right)\left(\Upsilon_{00} - \lambda\left(\Upsilon_{20} - \frac{n^2}{R}\Upsilon_{00}\right)\right) \quad (47)$$

$$k_{4,2} = -n\left(\frac{B_{12}}{R} + \frac{B_{66}}{R}\right)\left(\Upsilon_{20} - \lambda\left(\Upsilon_{40} - \frac{n^2}{R}\Upsilon_{20}\right)\right),$$
$$k_{2,4} = +n\left(\frac{B_{12}}{R} + \frac{B_{66}}{R}\right)\left(\Upsilon_{11} - \lambda\left(\Upsilon_{31} - \frac{n^2}{R}\Upsilon_{11}\right)\right) \quad (48)$$

$$k_{5,2} = B_{66}\left(\Upsilon_{20} - \lambda\left(\Upsilon_{40} - \frac{n^2}{R}\Upsilon_{20}\right)\right) - n^2\frac{B_{11}}{R^2}\left(\Upsilon_{00} - \lambda\left(\Upsilon_{20} - \frac{n^2}{R}\Upsilon_{00}\right)\right) + \frac{\tilde{A}_{66}}{R}\left(\Upsilon_{00} - \lambda\left(\Upsilon_{20} - \frac{n^2}{R}\Upsilon_{00}\right)\right), \quad (49)$$

$$k_{3,3} = \tilde{A}_{66}\left(\Upsilon_{20} - \lambda\left(\Upsilon_{40} - \frac{n^2}{R}\Upsilon_{20}\right)\right) - n^2\frac{\tilde{A}_{66}}{R^2}\left(\Upsilon_{00} - \lambda\left(\Upsilon_{20} - \frac{n^2}{R}\Upsilon_{00}\right)\right) - \frac{A_{11}}{R^2}\left(\Upsilon_{00} - \lambda\left(\Upsilon_{20} - \frac{n^2}{R}\Upsilon_{00}\right)\right) \quad (50)$$

$$k_{4,3} = \left(\tilde{A}_{66} - \frac{B_{12}}{R}\right)\left(\Upsilon_{20} - \lambda\left(\Upsilon_{40} - \frac{n^2}{R}\Upsilon_{20}\right)\right),$$
$$k_{3,4} = +\left(\frac{B_{12}}{R} - \tilde{A}_{66}\right)\left(\Upsilon_{11} - \lambda\left(\Upsilon_{31} - \frac{n^2}{R}\Upsilon_{11}\right)\right) \quad (51)$$

$$k_{5,3} = n\left(+\frac{\tilde{A}_{66}}{R} - \frac{B_{11}}{R^2}\right)\left(\Upsilon_{00} - \lambda\left(\Upsilon_{20} - \frac{n^2}{R}\Upsilon_{00}\right)\right),$$
$$k_{3,5} = -n\left(+\frac{B_{11}}{R^2} - \frac{\tilde{A}_{66}}{R}\right)\left(\Upsilon_{00} - \lambda\left(\Upsilon_{20} - \frac{n^2}{R}\Upsilon_{00}\right)\right) \quad (52)$$

$$k_{4,4} = +D_{11}\left(\Upsilon_{31} - \lambda\left(\Upsilon_{51} - \frac{n^2}{R}\Upsilon_{31}\right)\right) - n^2\frac{D_{66}}{R^2}\left(\Upsilon_{11} - \lambda\left(\Upsilon_{31} - \frac{n^2}{R}\Upsilon_{11}\right)\right) - \tilde{A}_{66}\left(\Upsilon_{11} - \lambda\left(\Upsilon_{31} - \frac{n^2}{R}\Upsilon_{11}\right)\right) \quad (53)$$

$$k_{5,4} = +n\left(\frac{D_{12}}{R} + \frac{D_{66}}{R}\right)\left(\Upsilon_{11} - \lambda\left(\Upsilon_{31} - \frac{n^2}{R}\Upsilon_{11}\right),\right),$$
$$k_{4,5} = -n(\frac{D_{66}}{R} + \frac{D_{12}}{R})(\Upsilon_{20} - \lambda(\Upsilon_{40} - \frac{n^2}{R}\Upsilon_{20})) \tag{54}$$

$$k_{5,5} = +D_{66}\left(\Upsilon_{20} - \lambda\left(\Upsilon_{40} - \frac{n^2}{R}\Upsilon_{20}\right)\right) - n^2\frac{D_{11}}{R^2}\left(\Upsilon_{00} - \lambda\left(\Upsilon_{20} - \frac{n^2}{R}\Upsilon_{00}\right)\right)$$
$$-\tilde{A}_{66}\left(\Upsilon_{00} - \lambda\left(\Upsilon_{20} - \frac{n^2}{R}\Upsilon_{00}\right)\right) \tag{55}$$

$$m_{1,1} = +I_0\Upsilon_{11} \tag{56}$$

$$m_{2,2} = m_{3,3} = m_{5,5} = +I_0\Upsilon_{00} \tag{57}$$

$$m_{4,1} = +I_1\Upsilon_{11},\ m_{4,4} = +I_2\Upsilon_{11}, \tag{58}$$

$$m_{5,2} = m_{2,5} = +I_1\Upsilon_{00} \tag{59}$$

$$Q_{load} = Q_n\Upsilon_{00} \tag{60}$$

where

$$\Upsilon_{00} = \int_0^L X_m X_m dx \tag{61}$$

$$\Upsilon_{20} = \int_0^L \frac{d^2X_m}{dx^2} X_m dx \tag{62}$$

$$\Upsilon_{11} = \int_0^L \frac{dX_m}{dx}\frac{dX_m}{dx} dx \tag{63}$$

$$\Upsilon_{31} = \int_0^L \frac{d^3X_m}{dx^3}\frac{dX_m}{dx} dx \tag{64}$$

$$\Upsilon_{40} = \int_0^L \frac{d^4X_m}{dx^4} X_m dx \tag{65}$$

For solving static ending problem of the nanoshell, the excitation frequency is set to zero. In the following, the normalized parameters and also suitable forms of function X_m have been introduced

$$\varpi = 100\omega_n h\sqrt{\frac{\rho_g}{E_g}}, \lambda = \frac{l}{L}, \qquad \bar{W}_{uniform} = W\frac{10E_c h^3}{L^4 q_0} \tag{66}$$

$$\mathrm{X}_m(x) = \sin\left(\frac{m\pi}{L}x\right) \tag{67}$$

The dynamical loading acted in the nanoshell may be defined as

$$q_{load} = \sum_{n=1}^{\infty} Q_n s\,in[\frac{m\pi}{a}x]\,cos[\,n\theta]\,sin\,\omega_{ex}\,t \tag{68}$$

$$\begin{aligned} Q_n &= \frac{1}{2\pi L}\int_{x_0-0.5L_0}^{x_0+0.5L_0}\int_{-\frac{\pi}{2}}^{\frac{3\pi}{2}} s\,in[\frac{m\pi}{L}x]\,cos[\,n\theta]\,q(x)dxd\theta \\ &= \frac{8q_0}{mn\pi^2}sin[\frac{m\pi}{L}x_0]\,sin[\frac{m\pi L_0}{2L}] \end{aligned} \tag{69}$$

So that $q(\mathrm{x}) = q_0$ defines the magnitude of uniform loading and x_0 is load position.

4. Discussions on results

The present section is concerned with the study of static/dynamic bending of crystalline porous nano-dimension shells taking into account strain gradient impacts. Also, in order to take into account small size effects much accurately, the surface energies related to grains and pores have been considered. In order to describe the material structure of crystalline shell, a micro-mechanical procedure is applied. A numerical trend was implemented in previous section to solve the governing equations and derive static and dynamic deflections. Based on strain gradient theory (SGT), Table 1 presents the verification of vibrational frequency of a nanoshell based on the data provided by Zeighampour and Beni (2014). The scale factor is selected to be l/h = 1 for this verification study. Further investigations are done for crystalline nanoshells based on the material properties provided in Table 2.

Table 1 Comparison of natural frequencies of strain gradient shells ($l = h$)

	ω_{11}		ω_{22}	
h/R	SGT (Zeighampour and Beni 2014)	present	SGT (Zeighampour and Beni 2014)	present
0.02	0.1980	0.1980	0.2795	0.2795
0.05	0.2110	0.2111	0.3953	0.3954

Table 2 Material properties of crystalline nanoshells

Phase-1 (Interface)	E_{in} = 45.56 GPa, v_{in} = 0.064, ρ_{in} = 2004.3 kg/m^3
Phase-2 (Si-nanograins)	E_g = 169 GPa, v_g = 0.064, ρ_g = 2300 kg/m^3
Phase-3 (nanovoids)	E_v = 0
Surface coefficients of grains and voids	λ_s = -4.488 N/m, μ_s = -2.774 N/m

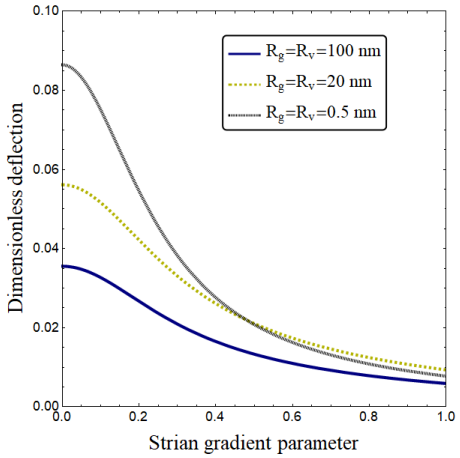

Fig. 3 Impact of grain sizes on dimensionless deflection variation of the nanoshell with respect to strain gradient coefficient (R/h = 20, f_v = 0.1)

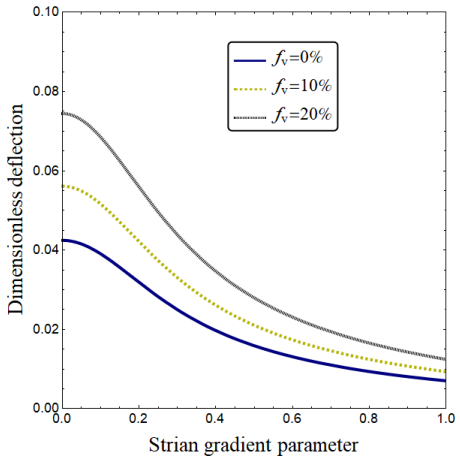

Fig. 4 Impact of pore percentage on dimensionless deflection variation of the nanoshell with respect to strain gradient coefficient (R/h = 20, Rg = 20 nm)

Fig. 3 illustrates the influences of the radius value of grains and pores on static bending deflection of the crystalline nanoshell with varying strain gradient coefficient (λ). The pore percentage value has been selected to be f_v = 10%. It is obvious from the figure that the shell deflection is reducing with increase of strain gradient coefficient which means that bending rigidity of the nanoshell is increasing. Hence, strain gradient coefficient plays an important role in static bending behavior of crystalline shells. Another finding form the figure is that increase of grain radius may increase the static deflection of the crystalline shell. Actually, the smallest value of bending deflection is obtained for R_g = 100 nm for which the crystalline shell is more rigid. So, the size of grains inside material will change bending behavior of the crystalline shell.

Pores percentage effects on static deflection of crystalline nanoshells is presented in Fig. 4 with varying strain gradient coefficient at R_g = 20 nm. Again, one can see that regardless of the amount

of pores, the shell deflection is reducing with increase of strain gradient coefficient which highlights the bending rigidity increment of the nanoshell. However, increase of pores percentage will increase the static deflection of crystalline shell. This means that bending rigidity of the crystalline shell has been reduced with increasing of pores percentage.

Fig. 5 explores the effects of radius-to-thickness ratios (R/h) of crystalline nanoshells on static deflections at R_q = 20 *nm* and f_v = 0.1. It is obvious form the figure that bending deflection is prominently increased by increasing of radius-to-thickness ratio. Such observation is owning to lower bending rigidity of the crystalline nanoshell as the radius-to-thickness ratios growth. As a conclusion, geometry of the nanoshell has great impact on its static bending behavior.

Influence of loading area (L_0/L) and location (x_0/L) on static deflections of crystalline nanoshells is plotted in Figs. 6 and 7, respectively. The pore percentage value has been selected to be f_v = 10%. It is obvious form the figure that as the transverse static load becomes far away from

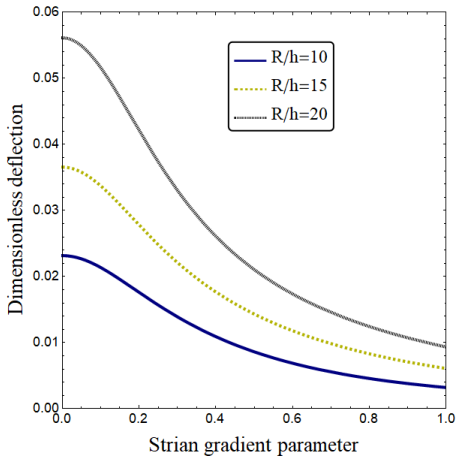

Fig. 5 Impact of shell radius on dimensionless deflection variation of the nanoshell with respect to strain gradient coefficient (*fv* = 0.1, R_g = 20 *nm*)

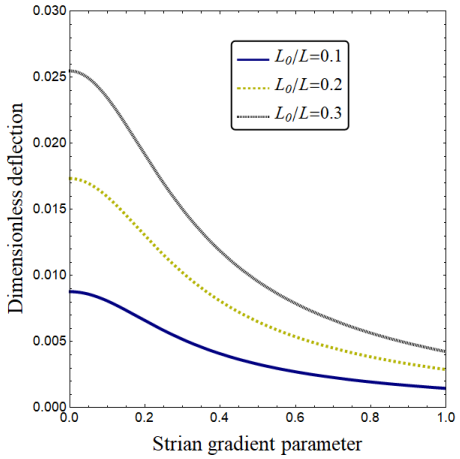

Fig. 6 Impact of dynamic load area on dimensionless deflection variation of the nanoshell with respect to strain gradient coefficient (x_0 = 0.5L, *fv* = 0.1, R_g = 20 nm)

the shell edges, the static deflections are lower. Actually, when the mechanical load is near the shell center, the static deflections growth. Also, as the area of transverse mechanical load is greater, the static deflections become larger.

Fig. 8 examine dynamic bending behavior of the crystalline shell having grain size of R_q = 100 nm for various values of strain gradient coefficient. Actually, this figure illustrates the dynamic deflection versus excitation frequency of dynamical load. According to this figure, it can be seen that the dynamic deflection of the crystalline shell is first increasing with increase of excitation frequency until a particular value of excitation frequency in which dynamic deflection is infinite. Such behavior is due to occurrence of resonance in the nanoshell related to its forced vibrations. The frequency in which the resonance occurs is dependent on the value of strain gradient coefficient. Actually, the resonance frequency is higher at larger values of strain gradient coefficient.

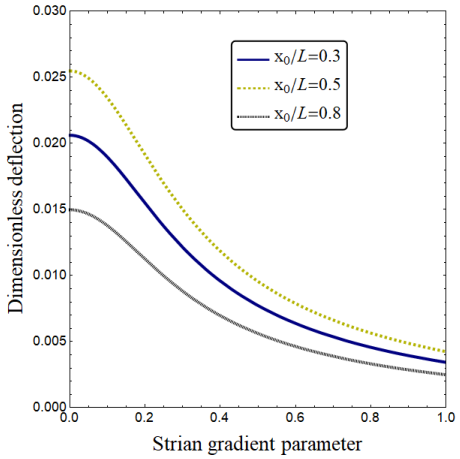

Fig. 7 Impact of dynamic load location on dimensionless deflection variation of the nanoshell with respect to strain gradient coefficient (L_0 = 0.3L, *fv* = 0.1, R_g = 20 nm)

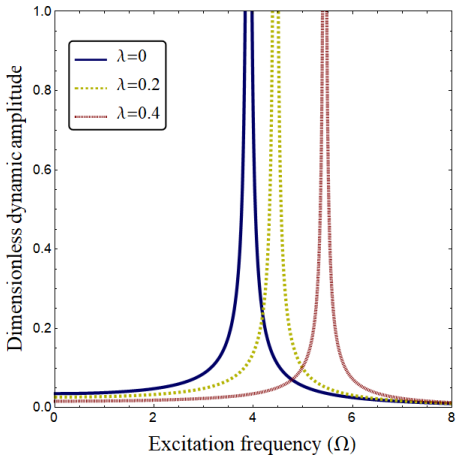

Fig. 8 Impact of strain gradient parameter on dimensionless deflection variation of the nanoshell with respect to excitation frequency (R/h = 20, R_g = 100 *nm*)

5. Conclusions

The presented article was concerned with the study of static/dynamic bending of crystalline porous nano-dimension shells taking into account strain gradient impacts. In order to take into account small size effects much accurately, the surface energies related to grains and pores were considered. In order to describe the material structure of crystalline shell, a micro-mechanical procedure was applied. A numerical trend was implemented to solve the governing equations and derive static and dynamic deflections. It was found that the shell deflection was reducing with increase of strain gradient coefficient which means that bending rigidity of the nanoshell was increasing. Another finding was that increase of grain radius may increase the static deflection of the crystalline shell. However, increase of pores percentage increased the static deflection of crystalline nanoshell.

Acknowledgments

The authors would like to thank Mustansiriyah university (www.uomustansiriyah.edu.iq) Baghdad-Iraq for its support in the present work.

References

Ahmed, R.A., Fenjan, R.M. and Faleh, N.M. (2019), "Analyzing post-buckling behavior of continuously graded FG nanobeams with geometrical imperfections", *Geomech. Eng., Int. J.*, **17**(2), 175-180. https://doi.org/10.12989/gae.2019.17.2.175

Al-Maliki, A.F., Faleh, N.M. and Alasadi, A.A. (2019), "Finite element formulation and vibration of nonlocal refined metal foam beams with symmetric and non-symmetric porosities", *Struct. Monitor. Maint., Int. J.*, **6**(2), 147-159. https:// doi.org/10.12989/smm.2019.6.2.147

Aydogdu, M. (2009), "A general nonlocal beam theory: its application to nanobeam bending, buckling and vibration", *Physica E: Low-dimens. Syst. Nanostruct.*, **41**(9), 1651-1655. https://doi.org/10.1016/j.physe.2009.05.014

Barati, M.R. (2017), "Nonlocal-strain gradient forced vibration analysis of metal foam nanoplates with uniform and graded porosities", *Adv. Nano Res., Int. J.*, **5**(4), 393-414. https://doi.org/10.12989/anr.2017.5.4.393

Barati, M.R. and Shahverdi, H. (2016), "A four-variable plate theory for thermal vibration of embedded FG nanoplates under non-uniform temperature distributions with different boundary conditions", *Struct. Eng. Mech., Int. J.*, **60**(4), 707-727. https://doi.org/10.12989/sem.2016.60.4.707

Barati, M.R. and Shahverdi, H. (2017a), "An analytical solution for thermal vibration of compositionally graded nanoplates with arbitrary boundary conditions based on physical neutral surface position", *Mech. Adv. Mater. Struct.*, **24**(10), 840-853. https://doi.org/10.1080/15376494.2016.1196788

Barati, M.R. and Shahverdi, H. (2017b), "Hygro-thermal vibration analysis of graded double-refined-nanoplate systems using hybrid nonlocal stress-strain gradient theory", *Compos. Struct.*, **176**, 982-995. https://doi.org/10.1016/j.compstruct.2017.06.004

Barati, M.R. and Shahverdi, H. (2017c), "Vibration analysis of multi-phase nanocrystalline silicon nanoplates considering the size and surface energies of nanograins/nanovoids", *Int. J. Eng. Sci.*, **119**, 128-141. https://doi.org/10.1016/j.ijengsci.2017.06.002

Barati, M.R. and Shahverdi, H. (2017d), "Frequency analysis of porous nano-mechanical mass sensors made of multi-phase nanocrystalline silicon materials", *Mater. Res. Express*, **4**(7), 075019. https://doi.org/10.1088/2053-1591/aa7ac2

Besseghier, A., Houari, M.S.A., Tounsi, A. and Mahmoud, S.R. (2017), "Free vibration analysis of embedded nanosize FG plates using a new nonlocal trigonometric shear deformation theory", *Smart Struct. Syst., Int. J.*, **19**(6), 601-614. https://doi.org/10.12989/sss.2017.19.6.601

Bounouara, F., Benrahou, K.H., Belkorissat, I. and Tounsi, A. (2016), "A nonlocal zeroth-order shear deformation theory for free vibration of functionally graded nanoscale plates resting on elastic foundation", *Steel Compos. Struct., Int. J.*, **20**(2), 227-249. https://doi.org/10.12989/scs.2016.20.2.227

Ebrahimi, F. and Barati, M.R. (2016), "Size-dependent thermal stability analysis of graded piezomagnetic nanoplates on elastic medium subjected to various thermal environments", *Appl. Phys. A*, **122**(10), 910. https://doi.org/10.1007/s00339-016-0441-9

Ebrahimi, F. and Barati, M.R. (2017a), "Vibration analysis of viscoelastic inhomogeneous nanobeams resting on a viscoelastic foundation based on nonlocal strain gradient theory incorporating surface and thermal effects", *Acta Mechanica*, **228**(3), 1197-1210. https://doi.org/10.1007/s00707-016-1755-6

Ebrahimi, F. and Barati, M.R. (2017b), "Size-dependent vibration analysis of viscoelastic nanocrystalline silicon nanobeams with porosities based on a higher order refined beam theory", *Compos. Struct.*, **166**, 256-267. https://doi.org/10.1016/j.compstruct.2017.01.036

Ebrahimi, F. and Barati, M.R. (2018), "Stability analysis of porous multi-phase nanocrystalline nonlocal beams based on a general higher-order couple-stress beam model", *Struct. Eng. Mech., Int. J.*, **65**(4), 465-476. https://doi.org/10.12989/sem.2018.65.4.465

Eltaher, M.A., Mahmoud, F.F., Assie, A.E. and Meletis, E.I. (2013), "Coupling effects of nonlocal and surface energy on vibration analysis of nanobeams", *Appl. Math. Computat.*, **224**, 760-774. https://doi.org/10.1016/j.amc.2013.09.002

Eringen, A.C. (1983), "On differential equations of nonlocal elasticity and solutions of screw dislocation and surface waves", *J. Appl. Phys.*, **54**(9), 4703-4710. https://doi.org/10.1063/1.332803

Farajpour, A., Rastgoo, A. and Mohammadi, M. (2017), "Vibration, buckling and smart control of microtubules using piezoelectric nanoshells under electric voltage in thermal environment", *Physica B: Condensed Matter*, **509**, 100-114. https://doi.org/10.1016/j.physb.2017.01.006

Ke, L.L., Wang, Y.S. and Wang, Z.D. (2012), "Nonlinear vibration of the piezoelectric nanobeams based on the nonlocal theory", *Compos. Struct.*, **94**(6), 2038-2047. https://doi.org/10.1016/j.compstruct.2012.01.023

Ke, L.L., Wang, Y.S. and Reddy, J.N. (2014), "Thermo-electro-mechanical vibration of size-dependent piezoelectric cylindrical nanoshells under various boundary conditions", *Compos. Struct.*, **116**, 626-636. https://doi.org/10.1016/j.compstruct.2014.05.048

Li, C. (2014a), "A nonlocal analytical approach for torsion of cylindrical nanostructures and the existence of higher-order stress and geometric boundaries", *Compos. Struct.*, **118**, 607-621. https://doi.org/10.1016/j.compstruct.2014.08.008

Li, C. (2014b), "Torsional vibration of carbon nanotubes: comparison of two nonlocal models and a semi-continuum model", *Int. J. Mech. Sci.*, **82**, 25-31. https://doi.org/10.1016/j.ijmecsci.2014.02.023

Li, C., Guo, L., Shen, J.P., He, Y.P. and Ju, H. (2013), "Forced Vibration Analysis on Nanoscale Beams Accounting for Effective Nonlocal Size Effects", *Adv. Vib. Eng.*, **12**(6), 623-633.

Li, L., Hu, Y. and Ling, L. (2016), "Wave propagation in viscoelastic single-walled carbon nanotubes with surface effect under magnetic field based on nonlocal strain gradient theory", *Physica E: Low-dimens. Syst. Nanostruct.*, **75**, 118-124. https://doi.org/10.1016/j.physe.2015.09.028

Lim, C.W. (2010), "On the truth of nanoscale for nanobeams based on nonlocal elastic stress field theory: equilibrium, governing equation and static deflection", *Appl. Math. Mech.*, **31**(1), 37-54. https://doi.org/10.1007/s10483-010-0105-7

Lim, C.W., Zhang, G. and Reddy, J.N. (2015), "A higher-order nonlocal elasticity and strain gradient theory and its applications in wave propagation", *J. Mech. Phys. Solids*, **78**, 298-313. https://doi.org/10.1016/j.jmps.2015.02.001

Mehralian, F., Beni, Y.T. and Ansari, R. (2016), "Size dependent buckling analysis of functionally graded piezoelectric cylindrical nanoshell", *Compos. Struct.*, **152**, 45-61. https://doi.org/10.1016/j.compstruct.2016.05.024

Mehralian, F., Beni, Y.T and Zeverdejani, M.K. (2017), "Nonlocal strain gradient theory calibration using molecular dynamics simulation based on small scale vibration of nanotubes", *Physica B*: *Condensed Matter*, **514**, 61-69. https://doi.org/10.1016/j.physb.2017.03.030

Merazi, M., Hadji, L., Daouadji, T.H., Tounsi, A. and Adda Bedia, E.A. (2015), "A new hyperbolic shear deformation plate theory for static analysis of FGM plate based on neutral surface position", *Geomech. Eng., Int. J.*, **8**(3), 305-321. https://doi.org/10.12989/gae.2015.8.3.305

Meyers, M.A., Mishra, A. and Benson, D.J. (2006), "Mechanical properties of nanocrystalline materials", *Progress Mater. Sci.*, **51**(4), 427-556. https://doi.org/10.1016/j.pmatsci.2005.08.003

Mokhtar, Y., Heireche, H., Bousahla, A.A., Houari, M.S.A., Tounsi, A. and Mahmoud, S.R. (2018), "A novel shear deformation theory for buckling analysis of single layer graphene sheet based on nonlocal elasticity theory", *Smart Struct. Syst., Int. J.*, **21**(4), 397-405. https://doi.org/10.12989/sss.2018.21.4.397

Saidi, H., Tounsi, A. and Bousahla, A.A. (2016), "A simple hyperbolic shear deformation theory for vibration analysis of thick functionally graded rectangular plates resting on elastic foundations", *Geomech. Eng., Int. J.*, **11**(2), 289-307. https://doi.org/10.12989/gae.2016.11.2.289

Shen, J.P., Wang, P.Y., Li, C. and Wang, Y.Y. (2019), "New observations on transverse dynamics of microtubules based on nonlocal strain gradient theory", *Compos. Struct.*, **225**, 111036. https://doi.org/10.1016/j.compstruct.2019.111036

Sun, J., Lim, C.W., Zhou, Z., Xu, X. and Sun, W. (2016), "Rigorous buckling analysis of size-dependent functionally graded cylindrical nanoshells", *J. Appl. Phys.*, **119**(21), 214303. https://doi.org/10.1063/1.4952984

Thai, H.T. (2012), "A nonlocal beam theory for bending, buckling, and vibration of nanobeams", *Int. J. Eng. Sci.*, **52**, 56-64. https://doi.org/10.1016/j.ijengsci.2011.11.011

Wang, G.F., Feng, X.Q., Yu, S.W. and Nan, C.W. (2003), "Interface effects on effective elastic moduli of nanocrystalline materials", *Mater. Sci. Eng.*: *A*, **363**(1), 1-8. https://doi.org/10.1016/S0921-5093(03)00253-3

Zaera, R., Fernández-Sáez, J. and Loya, J.A. (2013), "Axisymmetric free vibration of closed thin spherical nano-shell", *Compos. Struct.*, **104**, 154-161. https://doi.org/10.1016/j.compstruct.2013.04.022

Zeighampour, H. and Beni, Y.T. (2014), "Cylindrical thin-shell model based on modified strain gradient theory", *Int. J. Eng. Sci.*, **78**, 27-47. https://doi.org/10.1016/j.ijengsci.2014.01.004

Zenkour, A.M. and Abouelregal, A.E. (2014), "Vibration of FG nanobeams induced by sinusoidal pulse-heating via a nonlocal thermoelastic model", *Acta Mechanica*, **225**(12), 3409-3421. https://doi.org/10.1007/s00707-014-1146-9

Zhou, J.Q., Wang, L. and Ye, Z.X. (2013), "Micromechanics model for nanovoid growth in nanocrystalline materials", *Appl. Mech. Mater.*, **364**, 754-759. https://doi.org/10.4028/www.scientific.net/AMM.364.754

CC